Title

H-Ras Transformation of Mammary Epithelial Cells Induces ERK-Mediated Spreading on Low Stiffness Matrix

Journal

Advanced Healthcare Materials, 9(8)

ISSN

2192-2640

Authors

Plunkett, Christopher

Kumar, Aditya

Yrastorza, Jaime

et al.

Publication Date

2020-04-01

DOI

10.1002/adhm.201901366

Peer reviewed

HHS Public Access

Author manuscript

Adv Healthc Mater. Author manuscript; available in PMC 2021 April 01.

Published in final edited form as:

Adv Healthc Mater. 2020 April ; 9(8): e1901366. doi:10.1002/adhm.201901366.

H-Ras Transformation of Mammary Epithelial Cells Induces ERK-Mediated Spreading on Low Stiffness Matrix

Christopher Plunkett[1,‡], **Aditya Kumar**[1,‡], **Jaime Yrastorza**[1], **Yang-Hsun Hou**[1], **Jesse Placone**[1,†], **Gillian Grennan**[1], **Adam J. Engler**[1,2,3,*]

[1]Department of Bioengineering, UC San Diego; La Jolla, CA USA 92093

[2]Biomedical Sciences Program, UC San Diego; La Jolla, CA USA 92093

[3]Sanford Consortium for Regenerative Medicine; La Jolla, CA USA 92037

Abstract

Oncogenic transformation of mammary epithelial cells (MECs) is a critical step in epithelial-to-mesenchymal transition (EMT), but evidence also shows that MECs undergo EMT with increasing matrix stiffness; the interplay of genetic and environmental effects on EMT is not clear. To understand their combinatorial effects on EMT, pre-malignant MCF10A and isogenic Ras-transformed MCF10AT were cultured on polyacrylamide gels ranging from normal mammary stiffness, ~150 Pascals (Pa), to tumor stiffness, ~5700 Pa. Though cells spread on stiff hydrogels independent of transformation, only 10AT cells exhibited heterogeneous spreading behavior on soft hydrogels. Within this mixed population, spread cells exhibited an elongated, mesenchymal-like morphology, disrupted localization of the basement membrane, and nuclear localization of the EMT transcription factor TWIST1. MCF10AT spreading is not driven by typical mechanosensitive pathways including YAP and TGFβ or by myosin contraction. Rather, ERK activation induced spreading of MCF10AT cells on soft hydrogels and required dynamic microtubules. These findings indicate the importance of oncogenic signals, and their hierarchy with substrate mechanics, in regulating MEC EMT.

Graphical Abstract

[*]Correspondence: aengler@ucsd.edu, Phone: 858-246-0678, Fax: 858-534-5722.

Author Contributions

C.M.P., A.K., and A.J.E. conceived of the project and designed the experiments. C.M.P., A.K., J.Y., Y.H., G.G., and J.K.P. performed all cell assays. The manuscript was written by C.M.P., A.K., and A.J.E. with input from the other authors.

[†]Current Affiliation: Department of Physics and Engineering, West Chester University; West Chester, PA 19383 USA

[‡]Co-first authors

Supporting Information

Supporting Information containing 4 figures and 1 table is available from the Wiley Online Library or from the author.

Conflict of Interest

The authors declare no conflict of interest

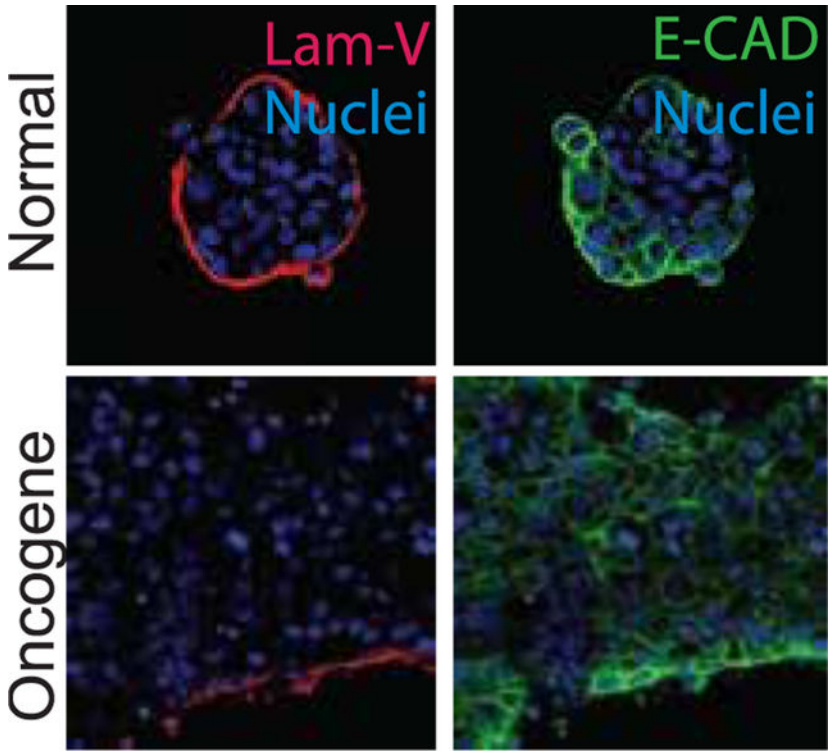

Oncogenes and material stiffness can facilitate the transformation of epithelial cells into mesenchymal cells, a process necessary for tumor formation. Their combined effect on this process, however, is unclear. Cells with and without expression of an oncogene, H-Ras, are cultured on substrates of normal and malignant mammary tissue. The oncogene can dominate mechanical signals from the adjacent material to drive cell transformation independent of material stiffness.

Keywords

gene-material interactions; breast cancer; H-ras; matrix stiffness; microtubules

1. Introduction

Carcinogenesis is a complex, multistep process that begins with the accumulation of mutations that transforms a healthy cell into a malignant one.[1] Genomic profiling has identified a number of oncogenes that are commonly mutated in tumors, but ascertaining their specific effects can be difficult as any given tumor may have combinations of multiple mutations within and between cells.[2] To reduce the complexity of heterogenous, multi-variant tumors, researchers have transformed cells with specific oncogenes to permit their isogenic interrogation.[3] For example, the Ras gene is commonly mutated in breast cancers, inducing increased cell proliferation, migration, and survival,[4] and to more easily examine its function, an H-Ras transformed clone, i.e. 10AT–referred to as 10AT, was created from pre-malignant mammary epithelial cells (MECs), i.e. 10A–referred to as 10A. Subsequently extensive genomic, transcriptomic, and proteomic analyses have been performed on these

paired cell lines, identifying several genes, such as c-myc, cyclins, and cell surface receptors, that are upregulated by Ras transformation.[5,6]

One classically defined pathway associated with H-Ras transformation involves the activation of extracellular signal-regulated kinase (ERK).[7] ERK activation has been shown to affect biological processes such as the dysregulation of cell proliferation and apoptosis and increased migratory propensity, thus highlighting the interest in studying this kinase in the cancer community. However, ERK activation appears to be cell and context specific, resulting in differences in downstream signaling and subsequent cell behavior.[8] In 10AT cells, ERK activation alone appears to be insufficient to induce migration and instead requires the additional activation of p38 or Y-box binding protein-1 to induce migration.[9,10] Thus, additional research is needed to understand ERK signaling as well as identification of downstream targets in various context.

The accumulation of genetic alterations is a well-established factor in tumor pathogenesis, although several other factors in the extracellular niche can also drive disease to varying effects. Extensive remodeling of the tumor microenvironment takes place during initiation, growth and metastasis of the tumor as well as its adjacent parenchyma. For example, mammary stroma experiences large increases in extracellular matrix (ECM) proteins, such as collagen and fibronectin, as well as increased crosslinking and fiber alignment, during tumor progression.[11] These changes increase ECM stiffness, which induces depolarization of mammary acini and invasion of MECs into the microenvironment.[12] A variety of potentially redundant mechanisms have been identified, namely epithelial to mesenchymal transition (EMT) through localization of the basic helix loop helix transcription factor Twist1[13] as well as activation of other mechanosensitive proteins such as YAP/TAZ and SMAD 2/3.[14] More recently, 3D culture of MECs on a soft but dynamic hydrogel results in acinar polarization that can be induced later to undergo EMT by stiffening the matrix; such dynamics more accurately models *in vivo* behavior and dramatic changes in morphology, gene expression, and response to drugs.[14–16] Conversely, *in vivo* ECM actually softens during therapeutic interventions such as radiation.[17]

Both oncogenic transformation and ECM stiffness contribute to tumor pathogenesis, but as outlined above, each has been largely observed independently of the other. Thus, we sought to understand the interplay of these factors by culturing the 10A cell lines on hydrogels that mimic stiffness ranging from that of healthy to malignant tissue. We hypothesized that as mutation burden increased, sensitivity to mechanical cues would concurrently decrease and lead to increased spreading at lower stiffness. While we specifically investigated the 10A and 10AT lines, this approach can easily be applied to other isogenic cell pairs to better understand this interplay in the context of different oncogenes and cancer types.

2. Results

2.1. H-Ras Transformation Induces Stiffness Insensitivity in Mammary Epithelial Cells

Elevated microenvironment stiffness induces invasive behavior in benign 10A MECs;[12] to determine whether malignant MECs show an altered sensitivity to niche stiffness, we cultured 10A cells and isogenic H-Ras transformed 10AT cells, as well as lines derived from

10AT xenografts, MCF10DCIS and MCF10CA1–referred to as 10DCIS and 10CA1, on polyacrylamide hydrogels ranging from physiologically soft (~150 Pa) to pathologically stiff (~5700 Pa) conditions. Typically MECs form large spheroids in 3D cultures or Matrigel overlaid 2D substrates and eventually hollow out with increasing maturity.[12] When substrate stiffness exceeded 670 Pa, all cell lines began to or exhibited complete loss of spheroid morphology and increased spread behavior (Supplemental Figure 1A). At or below 670 Pa, only 10AT spheroids exhibited morphologic changes (Figure 1A–B, Supplemental Figure 1A–B), with fewer spheroids and more spread cells in the surrounding environment compared to 10A cells (Figure 1C–D). While 10A response was largely homogeneous, whether circular or spread, the 10AT response on soft substrates was more heterogeneous owing to higher standard deviations in these metrics.

2.2. H-Ras Transformed Cells Undergo Heterogeneous EMT in a Soft Microenvironment

Cellular invasion of mammary stroma in stiff environmental conditions has been associated with an EMT transition whereby invading cells lose junction and basement membrane stability and adopt an elongated morphology.[18] To explore whether the spread 10AT cell population on soft hydrogels undergo aspects of EMT, we examined E-Cadherin and Laminin V expression on soft and stiff hydrogels to observe junctions and basement membrane, respectively. Whereas all cell lines showed a loss of Laminin V on stiff hydrogels (Figure 2A, Supplemental Figure 2A), only 10AT cells had destabilized basement membranes on all substrates (Figure 2A and Supplemental Figure 2A). To further explore the upstream EMT activators, we measured mRNA expression of five key transcription factors associated with EMT, Snail, Slug, Zeb1, Zeb2, and Twist1. This showed no significant differences in expression levels between groups (Supplemental Figure 2B), although it has been noted that transcriptional activity of some markers requires nuclear localization.[13,14] Thus we documented localization changes of Twist1, finding that in stiff conditions, it became nuclear localized for all cell lines (Figure 2B–C, Supplemental Figure 2C). However, for cells on soft substrates, 10AT was the only line to indicate Twist1 localization, albeit with remnants of spheroids exhibiting significant cytoplasmic Twist1 (Figure 2B–C). These data suggest that TWIST localization is not being driven by ECM stiffness in this context, so we examined other signaling molecules associated with the induction of EMT that have previously been implicated in mechanotransduction.[14,19,20] No increase in TGF-β mediated SMAD2/3 localization was detected within spread regions and TGF-β inhibition via Galunisertib did not prevent cells from spreading (Supplemental Figure 3A). Likewise, treatment with the YAP inhibitor Verteporfin did not prevent spreading (Supplemental Figure 3B). Thus, unlike in benign MECs, our data suggests that the spread subpopulation of H-Ras transformed cells exhibit EMT behavior on soft substrates via oncogene specific activation.

2.3. H-Ras Spreading in a Soft Microenvironment is Predicated Upon ERK Signaling and Microtubule Dynamics

Given the suggestion that H-Ras-mediated spreading is non-mechanotransductive, we next interrogated classic Ras pathway components, e.g. ERK activation,[7] to understand the effects in soft matrices. Whereas ERK activation increased for 10A cells cultured on stiff gels compared to those on soft, ERK was activated at far higher levels for 10AT cells

regardless of stiffness (Figure 3A–B). With high ERK activation independent of stiffness, we next determined whether 10AT spreading is ERK-dependent; cells were treated with the ERK inhibitor SCH772984 immediately upon or four days after seeding. On stiff substrates, ERK inhibition had no effect on cell spreading for either line (Figure 3C, Supplemental Figure 4A–C), which is consistent with activation of EMT-associated, mechanosensitive proteins. ERK inhibition dramatically reduced spreading of 10AT cells on soft conditions, but only when the drug was added from the outset (Figure 3C). To understand the downstream effects of ERK activation on the cytoskeletal organization–which regulates spreading, we treated cells with the microtubule inhibitors nocodazole (tubulin-binding) and paclitaxel (microtubule capping) and the myosin inhibitor blebbistatin. Microtubule remodeling inhibitors prevented 10AT cell spreading on soft substrates but induced a heterogeneous response for both 10A and 10AT cells on stiff substrates; a subset of the cells rounded up while the remaining cells spread (Figure 3D, Supplemental Figure 4D–G). No reduction in spreading was observed with blebbistatin, suggesting that actomyosin contraction is less involved in H-Ras- or stiffness-mediate cytoskeleton remodeling in MECs undergoing EMT (Figure 3D, Supplemental Figure 4D–G). Together these data imply an indirect pathway between H-Ras and MEK that turns on ERK phosphorylation and leads to changes in microtubule dynamics in a stiffness-independent manner (Figure 4).

3. Discussion

Understanding how oncogenes contribute to carcinogenesis is difficult due the inherent heterogeneity of tumors *in vivo*.[1,2] Oncogenic transformation of healthy cells has served as a powerful tool to understand mechanisms,[3] but since all cells sense their environment, it is important to understand to what extent stiffness can mediate EMT in the presence of an oncogene.[12–14,19] To illustrate this point, we demonstrated that H-Ras transformed MECs are insensitive to stiffness and adopt a partially spread phenotype on substrates with physiologically healthy stiffness. This spread cell fraction underwent EMT, allowing for increased migratory capacity via ERK-mediated microtubule dynamics.

Although H-Ras activation of ERK and subsequent microtubule polymerization has been demonstrated before,[21] this is the first study to demonstrate that ERK inhibition is sufficient to prevent H-Ras induced cell spreading on soft matrix. Interestingly, previous studies using H-Ras transformed 10A cells demonstrated that whereas p38 activation was sufficient to induce cell invasion in a transwell model,[10,22] ERK activation was not. These data highlight how specific matrix conditions, i.e. cell confinement during migration through a pore versus matrix stiffness, can induce different signaling pathways in transformed cell lines, which ultimately lead to nearly identical behaviors including cell spreading and migration. Interestingly and unlike with other extracellular signals, we found distinct subpopulations of H-Ras transformed cells that were or were not responsive to substrate stiffness, i.e. clustered or spread on soft substrates. Such heterogeneity is consistent with tumor behavior in patients and when cells are cultured on dynamic substrates where the specific amount of several signaling pathways could dictate more or less spheroid formation.[14] However observing heterogeneous responses within the 10AT line suggests some stochasticity in mechanotransduction pathways not directly assessed here. Aside from spreading, cytoskeletal remodeling downstream of ERK was also heterogeneous; application

of microtubule inhibitors on soft matrix reduced 10AT spreading but was less effective for both lines on stiff matrix. These data imply that H-Ras-mediated spreading was blocked on soft substrates but that stiffness-mediated spreading was only partially blocked on stiff substrates. While previously observed,[23] i.e. that there are overlapping mechanosensitive pathways,[14] these data highlight the importance of considering culture conditions in cell response. Given that even different RAS mutations can play different roles in cancer initiation compared to cancer progression,[24] observing how cells respond across the stiffness spectrum of cancer can provide insight into specific oncogene function.

4. Conclusions

These findings suggest that as tumors continue to develop and accumulate oncogenic mutation, the sensitivity of malignant cells may drive premature spreading behavior. It is therefore of great importance to identify and explore the role of other key mammary cell mutations such as BRCA1, B-RAF, or PI3K in altering stiffness sensitivity. These mutations may, through a similar mechanism, sensitize tumor masses to stiffness to differing degrees to permit destabilization of tumor spheroids and spreading.

5. Experimental Section

Cell Culture:

MCF10A and MCF10AT cells (referred to as 10A and 10AT, respectively) were expanded in DMEM/F12 media containing 5% horse serum, 20 ng/mL human EGF, 0.5 μg/mL hydrocortisone, 100 ng/mL cholera toxin, 10 ug/mL insulin, and 1% penicillin and streptomycin (Sigma-Aldrich). MCF10DCIS and MCF10CA1 were expanded in DMEM/F12 media containing 5% horse serum and 1% penicillin and streptomycin. Cells were detached when they reached 80% confluency using 0.05% trypsin for 7 minutes. Trypsin was neutralized using DMEM/F12 media containing 20% horse serum and cells were split 1:5 and reseeded. Cells were only used up to passage 10.

Polyacrylamide hydrogel synthesis:

Polyacrylamide gels were prepared as previously described.[25] 12 mm glass coverslips were methacrylated by first treating with UV-Ozone (BioForce Nanosciences) for 5 minutes followed by functionalization with 20 mM 3-(trimethoxysilyl)propyl methacrylate (Sigma-Aldrich) for 5 minutes. Hydrogel solutions were prepared by mixing acrylamide/bis-acrylamide solutions (Fisher) with 1% v/v of 10% ammonium persulfate (Fisher) and 0.1% v/v of N,N,N’,N’,-Tetramethylethylenediamine (VWR International). 3%/0.3%, 4%/0.3%, 3%/0.6%, and 5%/0.15% acrylamide/bis-acrylamide concentrations were used to achieve stiffness of 150, 320, 670, and 5700 pascal, respectively. 15 μL of solution was sandwiched between a functionalized coverslip and a dichlorodimethylsilane (Acros Organics)-coated glass slide. Polymerized gels were then washed with PBS and incubated with 0.2 mg/mL Sulfo-SANPAH in 50 mM HEPES pH 8.5 in the presence of 350 nm UV light (4 mW/cm^2, UVP) for 10 minutes, rinsed twice with PBS, and incubated overnight at 37°C with 0.15 mg/mL rat tail Collagen I (Millipore) in PBS. Gels were then rinsed with PBS and UV sterilized at 254nm for two hours at prior to use.

3-D Cell Culture:

Cells were seeded on hydrogels in the presence of 2% Matrigel (Corning) mixed with DMEM/F12 supplemented with 2% horse serum, 5 ng/mL human EGF, 0.5 mg/mL hydrocortisone, 100 ng/mL cholera toxin, 10 ug/mL insulin, and 1% penicillin and streptomycin. Cells were seeded on hydrogels at a density of 2000 cells per gel and allowed six days in culture to form mammary organoids. For drug experiments, cells were treated with SCH772984 (0.1–10 μM) either upon seeding or after 4 days of culture on hydrogels. Cells were dosed with nocodazole (0.05–2 μg/mL), paclitaxel (0.5–1 μg/mL), and blebbistatin (5–50 μM). Images were taken in 10x brightfield on day 6.

Morphological Analysis:

Brightfield images were acquired on a Nikon Eclipse Ti-S inverted microscope with a 10x objective and analyzed in ImageJ. Circularity was calculated by tracing cell boundaries and applying the following equation: Circularity = $4\pi(\text{area}/\text{perimeter})^2$. Percent acini was calculated by categorizing cells as either acinar or spread based on circularity and determining how many acinar regions remained. Spread cells per acini was calculated by counting the number of cells that migrated away from a specific acinus.

Immunofluorescence:

Cells were fixed with 3.7% formaldehyde for 15 minutes at room temperature. Matrigel was removed from samples by incubation in 5 mM EDTA (Fisher) for 30 minutes at 4°C. Samples were then permeabilized with PBS supplemented with $MgCl_2$ (final concentration 0.5 mM) (Solution A) and 0.5% Triton X-100 for 15 minutes at room temperature. Sample blocking was performed in a solution of 20% goat serum and 0.2% Triton-X 100 in Solution A for 30 minutes at room temperature. Primary antibodies were added and incubated overnight at 4°C. Dilutions were as follows: Anti-E-Cadherin (BD, cat # 610181, 1:50), Laminin V (abcam, cat # ab11575, 1:100), TWIST1 (Santa Cruz Biotechnology, cat # sc-81417, 1:25), and SMAD2/3 (Cell Signaling Technology, cat # D7G7, 1:1600). Samples were washed three times with Solution A for 5 minutes and subsequently incubated in secondary antibody solution (0.2% TritonX-100 and 20% Goat Serum in Solution A) at the following dilutions: Goat anti-mouse 488 (Invitrogen, A11004, lot 1218263, 1:500), Goat anti-rabbit 568 (A11011, Lot 1345045, 1:500) for 1 hour at room temperature. Samples were again washed three times for 5 minutes with Solution A and nuclei were counterstained with DAPI (Thermo, cat # D1306, 1:5000) in dH2O for 3 min. Hydrogels were mounted to glass slides using Fluoromount-G (Southern Biotech, cat # 0100–01) and allowed to dry for 1 hour after which gels were sealed with nail polish. Confocal images were taken on a Zeiss LSM 780 with a 40x water immersion objective.

For TWIST analysis, images were linearly analyzed in ImageJ and Zen software packages. Nuclear to cytoplasmic intensity ratios were calculated by first measuring the average nuclear fluorescent intensity for an individual cell and subsequently normalizing it to the same cell's average cytoplasmic fluorescent intensity. This process was carried out in both "Acini" and "EMT" regions as determined by the software operator for 10AT cells on soft substrates.

Western Blotting:

Western blot analysis was performed as described.[26] Briefly, cells were cultured on hydrogels for 6 days before lysis using RIPA buffer (50 mM HEPES, 150 mM NaCl, 1.5 mM $MgCl_2$, 1 mM EDTA, 1% Triton, 10% glycerol, 25 mM sodium deoxycholate, 0.1% SDS) containing Roche Complete Protease Inhibitor (Sigma-Aldrich) and PhosSTOP (Sigma-Aldrich). Protein concentrations of the samples were determined using a Pierce BCA Protein Assay kit (Thermo Scientific). 10 μg of protein from each sample was loaded into Bolt 4–12% Bis-Tris gels (Thermo) and separated by electrophoresis in MES running buffer (50 mM MES, 50 mM Tris Base, 1 mM EDTA, 0.1% w/v SDS) under reducing and denaturing conditions before being transferred onto a nitrocellulose membrane using the iBlot 1 semi-dry transfer system (Invitrogen). Membranes were incubated with 5% Seablock blocking buffer (Thermo) in Tris buffered saline with tween (150 mM NaCl, 15 mM Tris-HCl, 20 mM Tris Base, 0.1% Tween) for one hour followed by overnight incubation with either phosphorylated ERK (1:1000, Cell Signaling, cat # 9101) or total ERK (1:1000, Cell Signaling, cat # 9102) and Glyceraldehyde 3-phosphate dehydrogenase (1:7500 Abcam, cat # ab9484). Membranes were then incubated with Alexa Fluor 680 donkey anti-mouse (0.2 μg/mL, Thermo, cat # A10038) and Alexa Fluor 790 donkey anti-rabbit (0.2 μg/mL, Thermo, cat # A11374) for two hours. Blots were imaged using the Li-Cor Odyssey CLx imaging system (Li-Cor) and the integrated densities of bands were analyzed using the Li-Cor Image Studio Lite software.

Quantitative PCR:

To separate acini and spread cell regions, gels were mechanically dissected using a Zeiss Stereo Discovery. V8 for visualization. Resection of organoids was performed using a microdissection scalpel. Spread cell regions were then exposed to 0.05% Trypsin for 5 minutes to lift cells off the gels. RNA was isolated from these samples using Trizol-chloroform extraction per manufacturer's instructions (Thermo Fisher Scientific). cDNA was synthesized using 2 μg RNA and SuperScript III reverse transcriptase (Thermo Fisher Scientific) with random hexamer primers. Quantification (45 cycles, 95°C for 15 seconds followed by 60°C for 1 min) was carried out on a CFX384 Touch RT-PCR system (BioRad) with a SYBR Green probe (Thermo Fisher Scientific). Data were analyzed based on a standard curve generated from a fibronectin plasmid and all samples were normalized to GAPDH. Primers are listed in Supplemental Table 1.

Statistics:

Statistical significance was determined using a Student's t-test with Welch's correction or ANOVA with Tukey's post-hoc analysis as denoted. Analysis were performed using Graphpad Prism software, with the threshold for significance level set at $p<0.05$. All data is presented as mean ± standard deviation.

Supplementary Material

Refer to Web version on PubMed Central for supplementary material.

Acknowledgments

Funding for this work was provided by National Institutes of Health grants R01CA206880 (A.J.E.), R21CA217735 (A.J.E.), F32HL126406 (J.K.P.), and T32AR060712 (A.K.), Department of Defense grant W81XWH-13-1-0133 (A.J.E.), National Science Foundation grants 1463689 (A.J.E.) and 1763139 (A.J.E.) and the Graduate Research Fellowship program (A.K.), and the ARCS/Roche Foundation Scholar Award Program in the Life Science (A.K.).

References

[1]. SCOTT RE, WILLE JJ, WIER ML, Mayo Clin. Proc 1984, 59, 107. [PubMed: 6366382]

[2]. Di Nicolantonio F, Arena S, Gallicchio M, Bardelli A, Cell Cycle 2010, 9, 20. [PubMed: 20016269]

[3]. Elenbaas B, Spirio L, Koerner F, Fleming MD, Zimonjic DB, Donaher JL, Popescu NC, Hahn WC, Weinberg RA, Genes Dev. 2001, 15, 50. [PubMed: 11156605]

[4]. Zhao JJ, Gjoerup OV, Subramanian RR, Cheng Y, Chen W, Roberts TM, Hahn WC, Cancer Cell 2003, 3, 483. [PubMed: 12781366]

[5]. So JY, Lee HJ, Kramata P, Minden A, Suh N, Mol Cell Pharmacol 2012, 4, 31. [PubMed: 24558516]

[6]. Maguire SL, Peck B, Wai PT, Campbell J, Barker H, Gulati A, Daley F, Vyse S, Huang P, Lord CJ, et al., J. Pathol 2016, 240, 315. [PubMed: 27512948]

[7]. Liu F, Yang X, Geng M, Huang M, Acta Pharm. Sin. B 2018, 8, 552. [PubMed: 30109180]

[8]. Roberts PJ, Der CJ, Oncogene 2007, 26, 3291. [PubMed: 17496923]

[9]. Evdokimova V, Tognon C, Ng T, Ruzanov P, Melnyk N, Fink D, Sorokin A, Ovchinnikov LP, Davicioni E, Triche TJ, et al., Cancer Cell 2009, 15, 402. [PubMed: 19411069]

[10]. Kim MS, Lee EJ, Kim HRC, Moon A, Cancer Res. 2003, 63, 5454. [PubMed: 14500381]

[11]. Conklin MW, Eickhoff JC, Riching KM, Pehlke CA, Eliceiri KW, Provenzano PP, Friedl A, Keely PJ, Am. J. Pathol 2011, 178, 1221. [PubMed: 21356373]

[12]. Paszek MJ, Zahir N, Johnson KR, Lakins JN, Rozenberg GI, Gefen A, Reinhart-King CA, Margulies SS, Dembo M, Boettiger D, et al., Cancer Cell 2005, 8, 241. [PubMed: 16169468]

[13]. Wei SC, Fattet L, Tsai JH, Guo Y, Pai VH, Majeski HE, Chen AC, Sah RL, Taylor SS, Engler AJ, et al., Nat. Cell Biol 2015, 17, 678. [PubMed: 25893917]

[14]. Ondeck MG, Kumar A, Placone JK, Plunkett CM, Matte BF, Wong KC, Fattet L, Yang J, Engler AJ, Proc. Natl. Acad. Sci 2019, 116, 3502. [PubMed: 30755531]

[15]. Kenny PA, Lee GY, Myers CA, Neve RM, Semeiks JR, Spellman PT, Lorenz K, Lee EH, Barcellos-Hoff MH, Petersen OW, et al., Mol. Oncol 2007, 1, 84. [PubMed: 18516279]

[16]. Haagensen EJ, Thomas HD, Mudd C, Tsonou E, Wiggins CM, Maxwell RJ, Moore JD, Newell DR, Eur. J. Cancer 2016, 56, 69. [PubMed: 26820797]

[17]. Miller JP, Borde BH, Bordeleau F, Zanotelli MR, LaValley DJ, Parker DJ, Bonassar LJ, Pannullo SC, Reinhart-King CA, APL Bioeng 2018, 2, 031901. [PubMed: 31069314]

[18]. Lamouille S, Xu J, Derynck R, Nat. Rev. Mol. Cell Biol 2014, 15, 178. [PubMed: 24556840]

[19]. Dupont S, Morsut L, Aragona M, Enzo E, Giulitti S, Cordenonsi M, Zanconato F, Le Digabel J, Forcato M, Bicciato S, et al., Nature 2011, 474, 179. [PubMed: 21654799]

[20]. Meng Z, Qiu Y, Lin KC, Kumar A, Placone JK, Fang C, Wang K-C, Lu S, Pan M, Hong AW, et al., Nature 2018, 560, 655. [PubMed: 30135582]

[21]. Harrison RE, Turley EA, Neoplasia 2001, 3, 385. [PubMed: 11687949]

[22]. Shin I, Kim S, Song H, Kim HRC, Moon A, J. Biol. Chem 2005, 280, 14675. [PubMed: 15677464]

[23]. Rice AJ, Cortes E, Lachowski D, Cheung BCH, Karim SA, Morton JP, Del Río Hernández A, Oncogenesis 2017, 6, 1.

[24]. Miller MS, Miller LD, Front. Genet 2012, 2, 1.

[25]. Matte BF, Kumar A, Placone JK, Zanella VG, Martins MD, Engler AJ, Lamers ML, J. Cell Sci 2019, 132, jcs224360. [PubMed: 30559248]

[26]. Kumar A, Thomas SK, Wong KC, Lo Sardo V, Cheah DS, Hou Y-H, Placone JK, Tenerelli KP, Ferguson WC, Torkamani A, et al., Nat. Biomed. Eng 2019, 3, 137. [PubMed: 30911429]

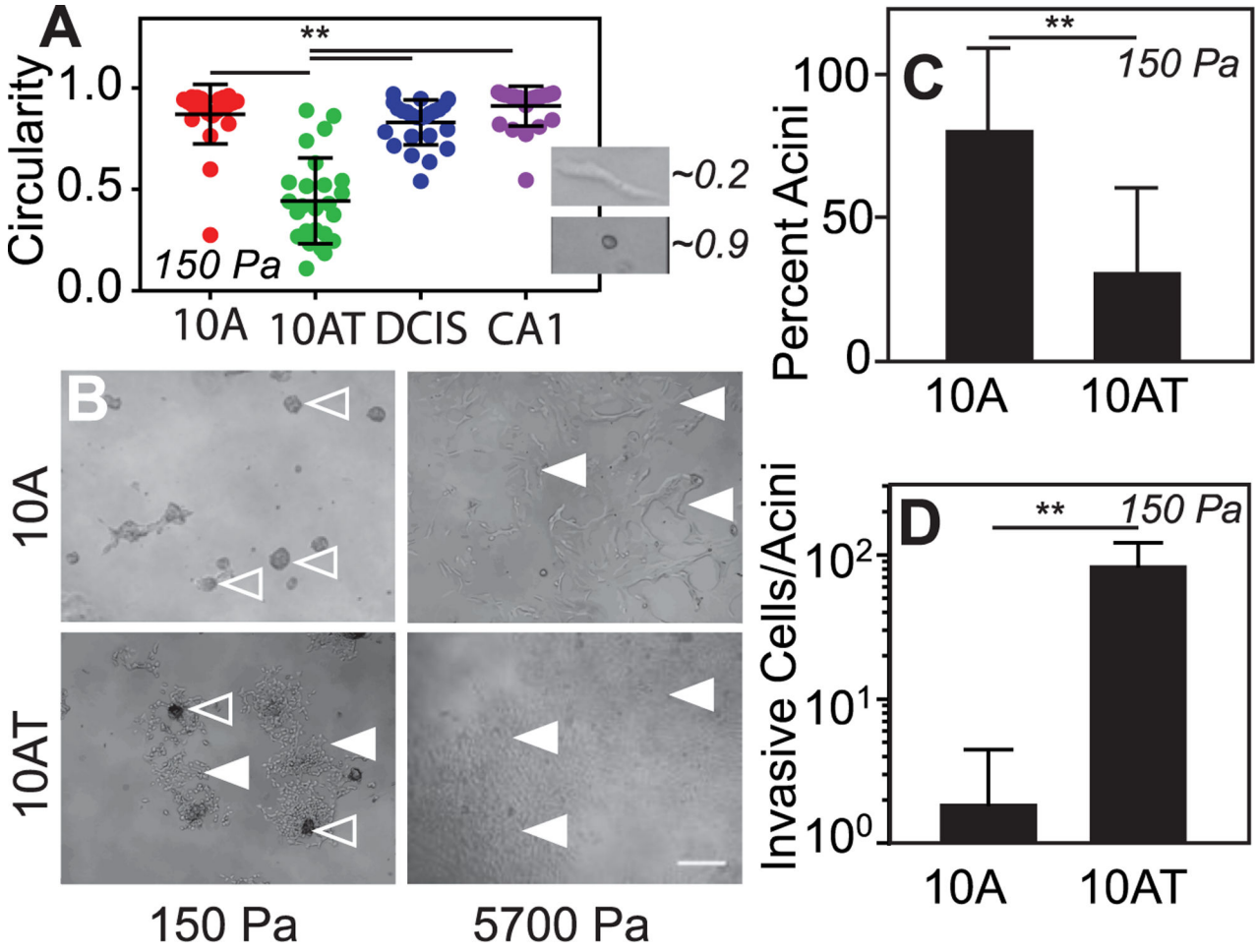

Figure 1: H-Ras transformed cells show heterogeneous spread behavior at physiologically soft mammary stiffness.

(A) Cell circularity for MECs on soft substrates. Inset demonstrates the circularity of different morphologies. **p<0.01, ANOVA with Tukey's post-hoc analysis. n = 3. **(B)** Brightfield images of MECs cultured on soft and stiff PA substrates. Hollow arrows indicated acini while solid arrows indicate spread regions. Scale bar is 250 μm. **(C)** Total percentage of acini present per hydrogel on soft substrates for each MEC line. **p<0.01, unpaired t-test with Welch's correction. n = 3. **(D)** Average number of spread cells produced per acini on soft substrates. **p<0.01, unpaired t-test with Welch's correction. n = 3.

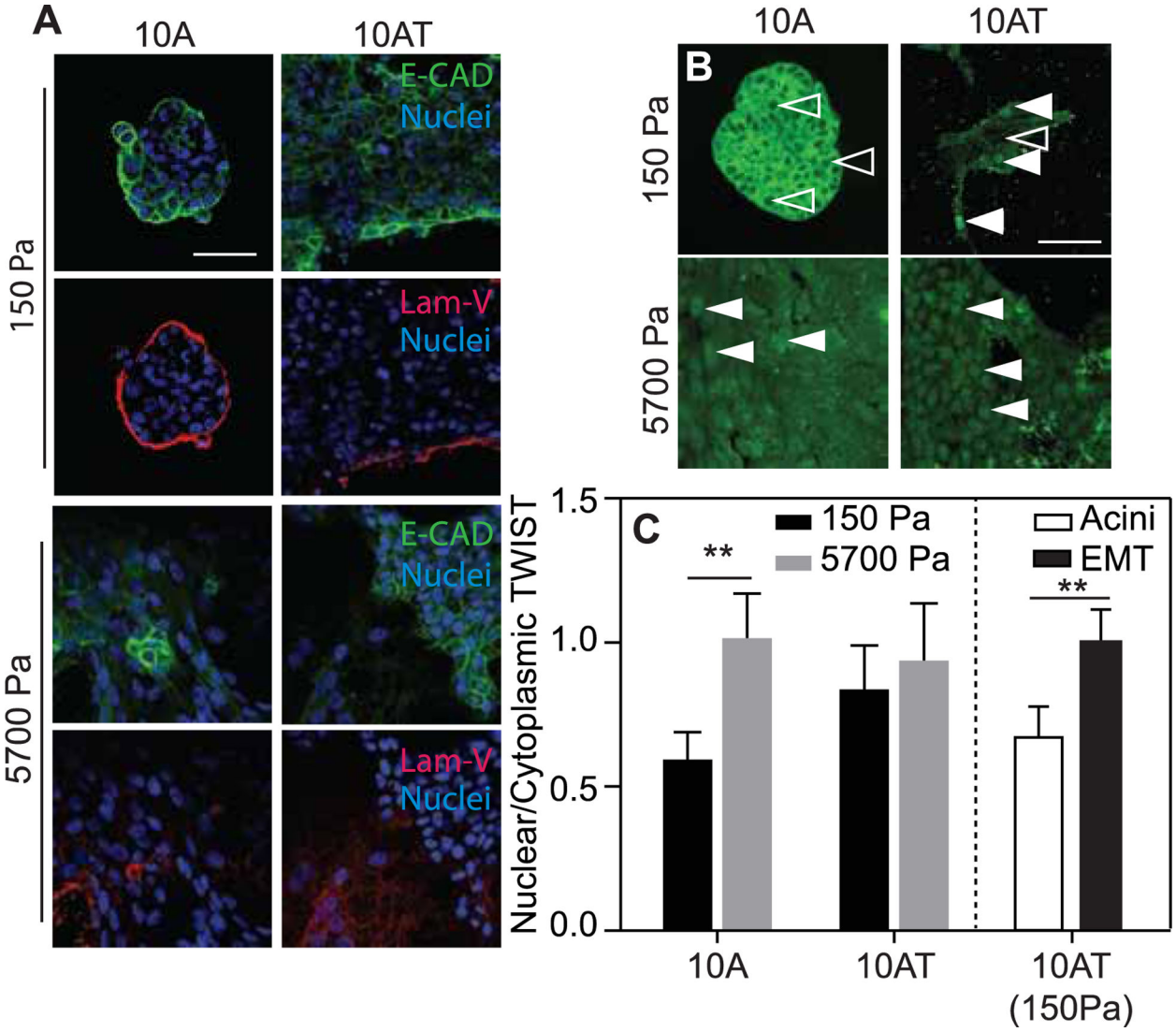

Figure 2: Spread subpopulations of H-Ras transformed cells undergo EMT on soft substrates.

(A) Immunofluorescent staining for E-Cadherin (green), Laminin V (red) and DAPI (blue). Scale bar is 50 μm. **(B)** Immunofluorescent staining of TWIST1 where hollow arrows indicate non-nuclear localizing transcription factor while solid arrows indicate localized transcription factor. Scale bar is 50 μm. **(C)** TWIST nuclear-to-cytoplasmic fluorescent intensity ratio. Right black and white bars show the ratio for 10AT cells in acinar (left bar) or mesenchymal-like structures (right bar) on soft hydrogels. **p<0.01, non-paired t-test with Welch's correction. n = 3.

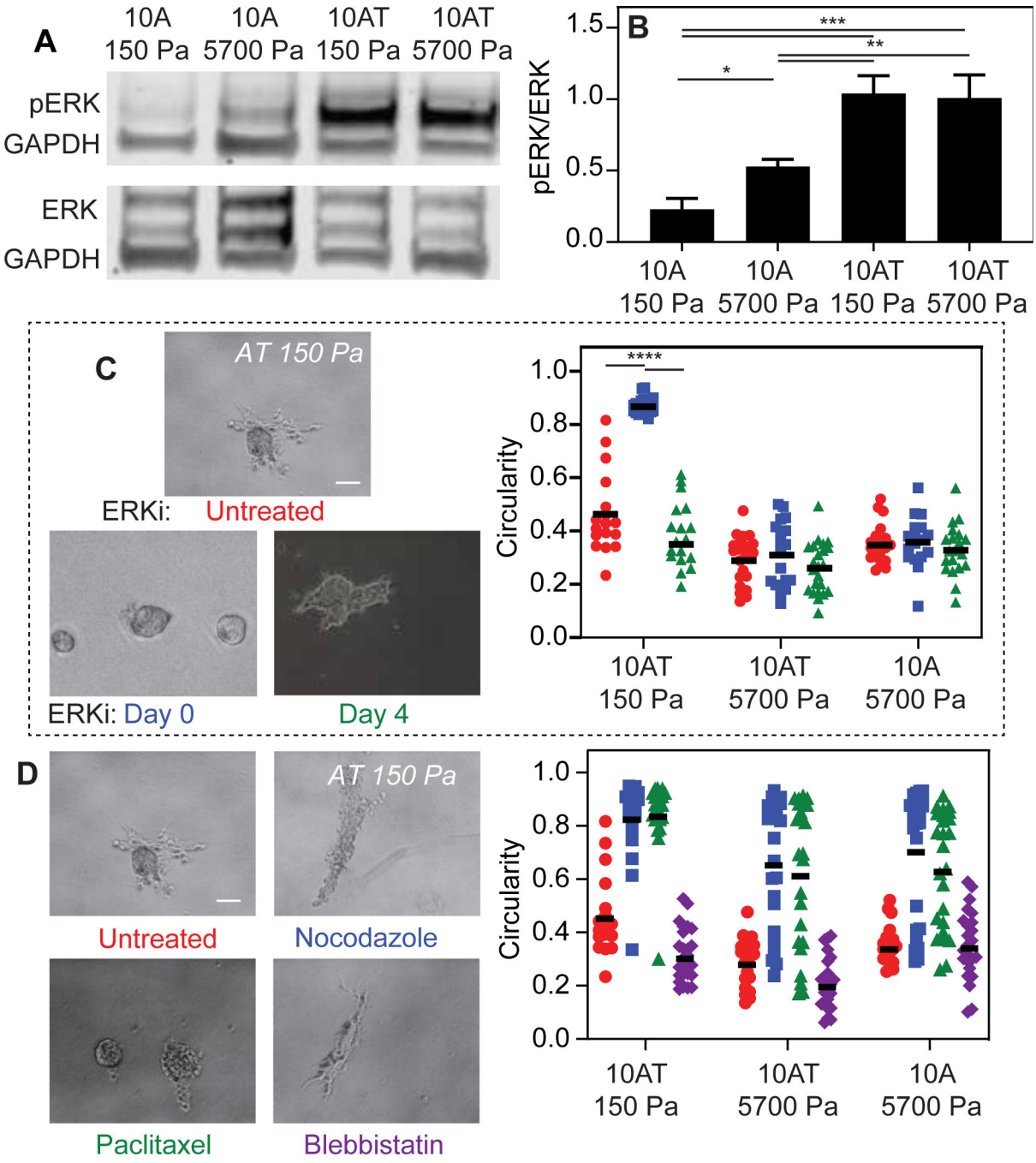

Figure 3: H-Ras Induces ERK-Mediated Spreading Via Microtubule Polymerization.

(A) Western blots showing phosphorylated and total ERK expression for cell lines on different stiffness. Values were normalized to GAPDH expression as a loading control and plotted in panel **B**. *p<0.05, *p<0.01, ***p<0.001, ANOVA with Tukey's post-hoc analysis. n=3. **(C)** Brightfield images of 10AT spheroids on soft substrates that are either untreated or treated with ERK inhibitor at the time of seeding or after four days of culture. Cell circularity for lines on different stiffness and drug timing are plotted with a bar representing the mean. ****p<0.0001, ANOVA with Tukey's post-hoc analysis. n=3. Scale bar 100 μm.

(**D**) Brightfield images of 10AT spheroids on soft substrates that are either untreated or treated with microtubule and myosin inhibitors and cell circularity for cell lines on different stiffness and drugs. Scale bar 100 μm.

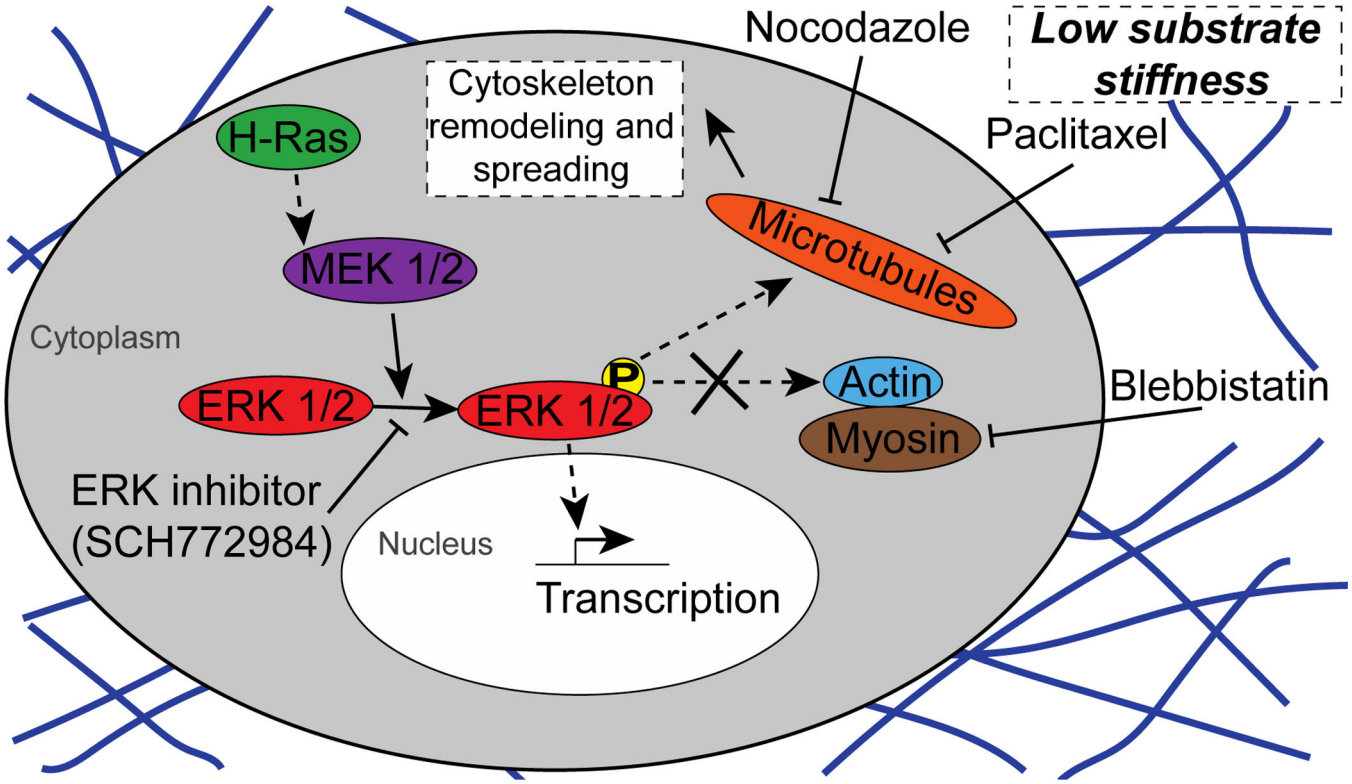

Figure 4: Schematic of 10AT signaling on low stiffness substrates.

Unlike on stiff substrates where cells mechano-sense, active H-Ras signaling on soft substrates in 10AT cells leads to downstream activation of MEK 1/2 and subsequently ERK 1/2 phosphorylation. Downstream targets of ERK 1/2 are implicated in cell proliferation, cytoskeleton rearrangement and preventing cell death. Inhibition of ERK phosphorylation prevents spreading on low stiffness substrates. Downstream of ERK, cytoskeletal assembly, which impacts cell spreading, is differentially responsive: inhibition of microtubule dynamics via nocodazole and paclitaxel, but not actomyosin dynamics with blebbistatin, prevents spreading of H-Ras transformed cells.